Stability, Electronic and Optical Properties of In-plane WSe_2 Heterophase Nano-ribbons

Ankush Bharti[1, a)] Neha Katoch[2] Ashok Kumar[3] Raman Sharma[1,b)] and PK Ahluwalia[1]

[1]*Department. of Physics, Himachal Pradesh University, Shimla, H. P., 171005 (India)*
[2]*Department. of Physics and Astronomical Science, School of Physics and Material Sciences, Central University of Himachal Pradesh University, Dharamshala, Kangra H. P., 176215 (India)*
[3]*Department. of Physical Science, School of Basic and Applied Sciences, Central University of Punjab, Bathinda, 151001 (India)*

Corresponding Author: [a)] bhartiankush7@gmail.com, [b)] bramans70@yahoo.co.in

Abstract. We present first principle investigations on in-plane phase engineered nanoribbons with two different widths. 2H and 1T' phases of WSe_2 are joined along x-direction, which forms an armchair type interface. The low values of formation energy shows that these structure are energetically stable. The study of electronic structure reveals that they are metallic and the electronic conductivity varies significantly with ribbon length. The ribbons show anisotropic dielectric response compared to constituent monolayers. Optical properties alter considerably for these hetero-systems showing potential for tunable opto-electronic applications.

INTRODUCTION

2D materials such as Graphene, h-BN, TMD's and X-enes (X=Si, Ge, Sn & P, As, Sb, Bi) have emerged as potential candidates for future nano-scale devices with exceptional functionalities aided by polymorphic nature. They possess unique properties like exceptional mechanical strength and thermal conductivity, superior flexibility, ultra-high carrier mobilities, tunable band gaps, quantum spin Hall insulation (QSH) etc. owing to the confined flow of heat and charge in two-dimensions.

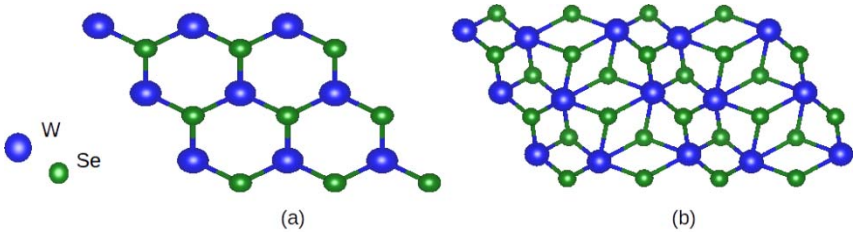

Figure 1. Schematic Models of single layered (a) 2H phase and (b) 1T' phase of WSe_2 respectively.

These serve as building blocks for atomically thin integrated circuitry because of different stacking possibilities leading to many complex device designs. Two basic types of possible integrations are termed as vertical (Van der Waals heterostructures) and lateral or in-plane heterostructures. In a study of vertical heterostructres based on (α, β) phosphorene and (H, T, ZT) phases of $MoSe_2$, the Schottky Barrier Height (SBH) is tuned to zero by external negative electric field of around -1.0 $VÅ^{-1}$ [1].

Recent study on vdW heterosystems of MX_2 with different phases of phosphorene shows the upper limit energy conversion efficiencies upto 1.16% and 0.98 % [2]. It is therefore worth exploring the basic properties of the

DAE Solid State Physics Symposium 2018
AIP Conf. Proc. 2115, 030360-1–030360-4; https://doi.org/10.1063/1.5113199
Published by AIP Publishing. 978-0-7354-1851-6/$30.00

heterostructures, like stability, description of mid-gap states, optical response to get deeper understanding of their properties. Lateral type hetero-structures have advantage of small lattice mismatch and covalent bonding at the interface leading to seamless, sharp and clean contact [8]. In the present work, we systematically model in-plane hetero phase ribbons of 2H and 1T' phases of WSe_2. Two geometries of nano-ribbons, in which 5×5 cells and 7×7 cells of 2H and 1T' phase are joined along x-axis forming armchair-type (AC) interfaces are studied. Structural stability is discussed using formation energy. Finally, electronic and optical properties of the optimized nano-ribbons are discussed in detail.

COMPUTATIONAL DETAILS

All the calculations have been performed in SIESTA simulation package [5]. GGA-PBE functional has been employed for the description of correlation and exchange interaction between electrons. Double zeta basis set with polarization functions (DZP) is used to expand Kohn-Sham orbitals. Structures were relaxed until each atom has forces less than 0.01 eV $Å^{-1}$. Brillouin zone was sampled with k-point mesh of $20 \times 20 \times 1$ and $30 \times 30 \times 1$ for 2H and 1T' phases of WSe_2 and heterostructrues respectively. Real space was sampled with 400 Ry of mesh cutoff energy for 2H,1T phases and their heterosturcture. Vacuum of 20 Å was used to avoid interactions between periodic images. The static dielectric constant ($\boldsymbol{\varepsilon_s}$) is calculated as the value of dielectric function at zero frequency for the real part.

RESULTS AND DISCUSSIONS

Structure and Stability

We have optimized two different configurations, one having five 2H and 1T' cells (5 × 5 hetero nanoribbon) and other having seven 2H and 1T' cells (7×7 hetero nanoribbons) as shown in fig. 2 (a). Hexagonal arrangement across the junction remains intact. We have calculated the formation energy per interface length for each ribbon. The formation energy can be defined as the energy required to assemble the hetero nano-ribbons and this energy can be obtained by the following equation:

$$E_f = [E_{hybrid} - N_W \times E_W - N_{Se-2H} \times E_{Se-2H} - N_{Se-1T'} \times E_{Se-1T'}]/L$$

Here E_{hybrid} is the total energy of optimized hetero system. N_W is the number of W atoms in the system. E_W is the free energy of the W atom. N_{Se-2H} and $N_{Se-1T'}$ are the no. of Se atoms in the 2H side and 1T side of the hetero system respectively. E_{Se-2H} and $E_{Se-1T'}$ are energies per atom of Se in pristine 2H and 1T' phase respectively. L is the width of the ribbon. The obtained E_f for both the ribbons (0.068, 0.037 eV) respectively are one order lower than reported value (0.22 eV/Å) for graphene/h-BN in-plane AC interface [3]. This shows that these heterostructures can readily be formed. Smaller values can be attributed to similar atomic environment across the interface.

TABLE 1. Lattice Parameters (a,b), Formation energy (E_f) for monolayers and heterostructures. Static dielectric constants for polarization along x ($\boldsymbol{\varepsilon_s^x}$) and for polarization along y-direction ($\boldsymbol{\varepsilon_s^y}$) are also given.

	Monolayers			**Heterostructures**	
Parameters	**2H-WSe_2**	**1T'-WSe_2**		**2H+1T' (5×5)**	**2H+1T'(7×7)**
			Ribbon		
a, b (Å)	3.35, 3.35	6.88, 3.34	**Width (Å)**	71.57	91.45
E_f (eV)	-	-		0.068	0.037
$\boldsymbol{\varepsilon_s^x}$	4.79	61.71		25.61	35.29
$\boldsymbol{\varepsilon_s^y}$	4.79	79.48		41.13	71.55

Electronic Properties

Electronic Structure of ribbons is found to be influenced by the mid gap states arising at the interface and edge reconstruction of ribbons. The ribbons attain metallic character and the metallicity is mainly due to 5d electrons of W and 4s electrons of Se in 5×5 ribbon. In 7×7 ribbon, it is due to 5d electrons of W and 4p electrons of Se respectively. The general character of band dispersion and no. of bands crossing Fermi level is dependent on ribbon width.

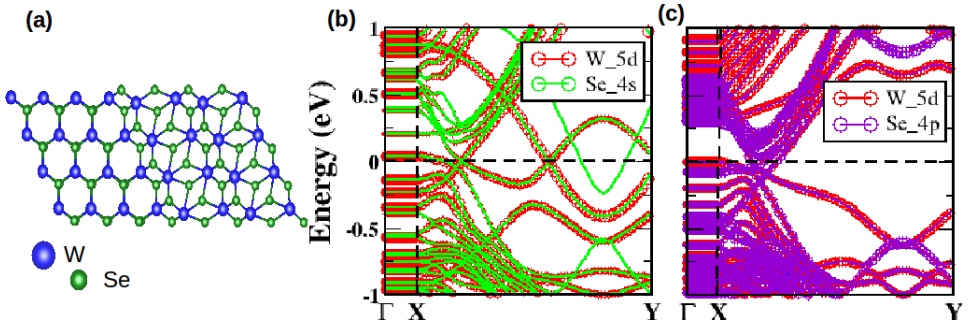

Figure 2. (a) Relaxed Structure of heterophase nanoribbon based on WSe_2. (b) Orbital resolved band structure for 5×5 ribbon. Red and green color are depicting contribution from 5d of W and 4s orbitals of Se respectively. (c) Band structure for 7×7 ribbon. Red and violet color indicating contribution from 5d of W and 4p of Se respectively.

Thus the conductivity can be tuned with ribbon width. The additional states due to interface act as reservoir for charge transfer processes which may be useful in formation of p-n junctions and SBH engineering [7].

Dielectric Properties

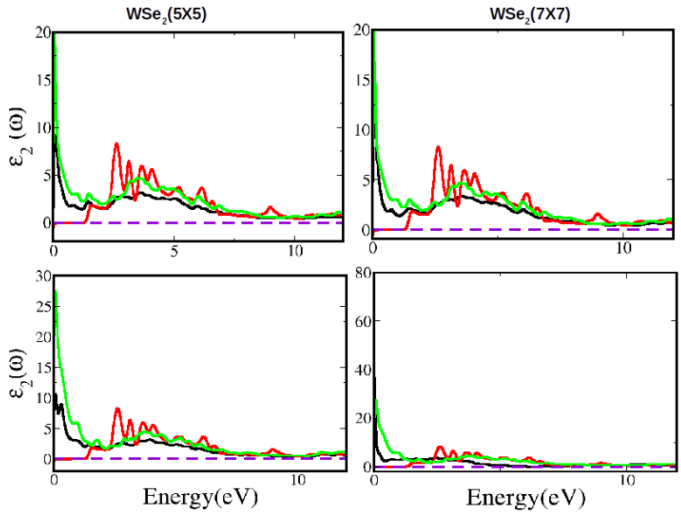

Figure 3. Imaginary part of dielectric function ($\boldsymbol{\varepsilon_2}$) for 5×5 and 7×7 ribbons. Red and green color are dielectric functions for constituent 2H and 1T' sheets respectively for comparison.Two curves (vertically downwards) for each ribbon is showing dielectric constant for polarization along x and y respectively.

Dielectric response of ribbons is determined for polarization along x and y-direction and compared with pristine phases. The calculated static dielectric constant ($\boldsymbol{\varepsilon_s}$) of monoloyers is small and of ribbons is large. High value of dielectric constant refers to metallic system, also confirmed by the Drude peak at (0 eV) in imaginary part of dielectric function for 1T' phase and ribbons. In imaginary part, first excitation peak for 2H is obtained at (1.59 eV) consistent with experimental value [4]. For 1T' phase and ribbons, we also observed red shift showing the decrease in band gap, which can also be confirmed from the band diagram.

Optical Properties

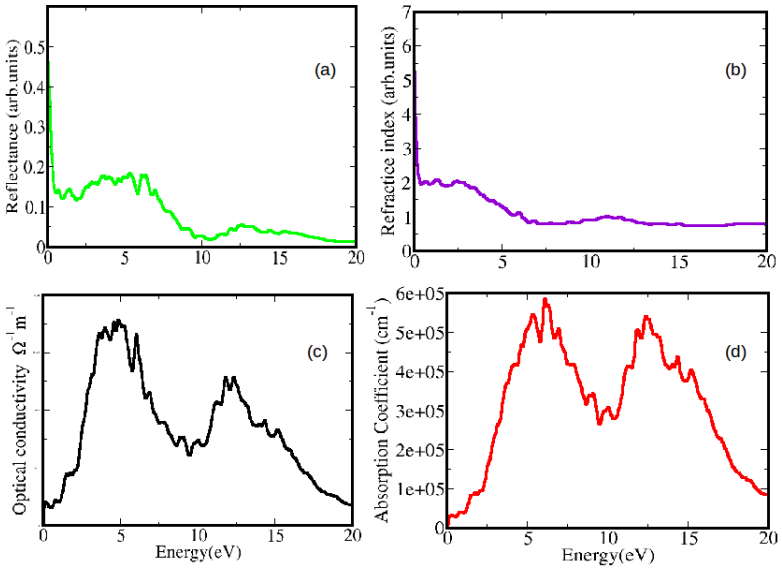

Figure 4. (a) Calculated Reflectance (b) Refractive index (c) Optical Conductivity and (d) Absorption coefficient for 7×7 ribbon with polarization along x-direction.

We calculated optical properties for 7×7 ribbon and found that Reflectance, Refractive index, optical conductivity and absorption co-efficient are altering in both visible (1.59-3.26 eV) and UV (3.26-12.4 eV) region. Reflectance is high in infra-red region (0.8-1.58 eV) but decreases for visible regions. In visible region, low absorption and low reflectance shows applications in antireflective coating materials used in solar cells [6].

CONCLUSIONS

In summary, we have investigated heterophase nano-ribbons using DFT. Low formation energies show the stability of hetero-interface. As hexagonal arrangement of atoms is not disturbed across the ribbon, they are forming seamless and sharp contact. Electronic properties show transition towards metallic 1T' region and are found to depend on ribbon width. Anisotropic dielectric and optical response shows that optical properties can be tuned with in-plane phase engineering. Present results provide insights for more experimental work in the field of in-plane phase engineering for future nano-electronics and opto-electronics.

ACKNOWLEDGEMENTS

We gratefully acknowledge National Supercomputing Facility at CDAC-PUNE, SIESTA team for code and HPC facility sponsored by DST under FIST program in Physics Department of Himachal Pradesh University, Shimla.

REFERENCES

1. K. Sumandeep et.al., Physical Chemistry Chemical Physics **19**(33),22023-22032 (2017).
2. Peng, Qiong, et. al., Scientific Reports **6**,31994 (2016).
3. Zhang, Junfeng, et al., Chemistry of Materials **28**(14),5022-5028 (2016).
4. Amin, Bin, et al., Applied Physics Letters **108**(6),063105 (2016).
5. Soler, J.M., Artacho et al., Journal of Physics: Condensed Matter 14(11), 2745 (2002).
6. Lu, X.,Lei, Q.,Gao et al., physica status solidi (b), 2018.
7. Paz, W. S., & Palacios, J.J., 2D Materials, **4**(1), 015014 (2016).
8. Fan, Z.Q., Jiang, X. W. et al., ACS applied materials & interfaces, 2018.